Spectrum of Engineering Sciences
ISSN (e) 3007-3138 (p) 3007-312X Volume 3, Issue 10, 2025

# GREEN SYNTHESIS OF SILVER NANOPARTICLES USING CHIA (*SALVIA HISPANICA* L.) SEED MUCILAGE AND THEIR ANTIOXIDANT, ANTIDIABETIC, AND ANTI-INFLAMMATORY ACTIVITIES

**Muhammad Waqar[1], Rashid Mahmood[*2], Nasir Assad[*3], Hassan Ali[4], Yasir Assad[5], Jaffar Irfan[6] Muhammad Tahir Akhtar[7]**

[1, *2,] *Faculty of Sciences, Superior University Lahore, Lahore 54000, Pakistan.*
[*3,6,7] *Institute of Chemistry, University of Sargodha, Sargodha 40100, Pakistan*
[4]*Department of Physics, University of Agriculture Faisalabad, Faisalabad 38040, Pakistan*
[5]*Department of Zoology, Hazara University, Mansehra, Pakistan*

[1]muhammadwaqar717157@gmail.com, [*2]rashid.mahmood.sgd@superior.edu.pk, [*3]nakhan_98@yahoo.com, hassanali20ag4374@gmail.com, [5]yasirassad01@gmail.com, [6]jaffarirfanchemist@gmail.com, [7]tahir_chemist14@yahoo.com

DOI:https://doi.org/10.5281/zenodo.17645992

**Keywords**
*Green synthesis, Silver nanoparticles, Chia seeds, Antioxidant activity, Antidiabetic activity, Anti-inflammatory activities*

**Article History**
*Received: 11 September 2025*
*Accepted: 21 October 2025*
*Published: 04 November 2025*


**Corresponding Author: ***
**Rashid Mahmood**
**Nasir Assad**

**Abstract**

*This study investigates the green synthesis of silver nanoparticles (AgNPs) using chia (Salvia hispanica L.) seed mucilage and evaluates their antioxidant, antidiabetic, and anti-inflammatory activities. The synthesis of AgNPs was confirmed by UV-Vis spectroscopy, which showed a characteristic surface plasmon resonance (SPR) peak at 426 nm, indicating successful NPs formation. Scanning electron microscopy (SEM) revealed spherical, well-distributed NPs with a mean size of 82.02 ± 2.7 nm, confirming the controlled size and morphology of the synthesized AgNPs. The antioxidant potential was assessed through DPPH and FRAP assays, where SH@AgNPs demonstrated significant radical scavenging and ferric ion-reducing activities, comparable to ascorbic acid. The antidiabetic activity was measured using an α-amylase inhibition assay, with SH@AgNPs achieving up to 45.71% inhibition at 30 µg/mL. Additionally, enzyme kinetics analysis showed a dose-dependent increase in α-amylase inhibition. The anti-inflammatory activity was tested using an egg albumin denaturation model, where SH@AgNPs exhibited up to 78.56% inhibition, approaching the 83.18% inhibition observed with Diclofenac sodium. These findings highlight the promising biological activities of SH@AgNPs, supporting their potential as multifunctional therapeutic agents for antioxidant, antidiabetic, and anti-inflammatory applications. The green synthesis method not only offers a sustainable and cost-effective approach but also results in biocompatible NPs suitable for further biomedical investigations.*

## INTRODUCTION

Nanotechnology is an emerging and rapidly developing field of science and technology dedicated to manipulate matter at the molecular and atomic level in the nanometer (1-100 nm), which leads into

preparation of new materials and devices with novel or even unattainable properties compared with those produced in bulk [1]. The synthesis of nanoparticles (NPs), one of the most important areas in nanotechnology, has received widespread applications including medicine, electronics, energy, and environmental sciences [2]. Among a variety of NPs, Metal NPs have attracted considerable attention because of their special chemical, physical, and optical properties that depend on their size, shape, high surface and volume ratio [3].

Among MNPs, silver nanoparticles (AgNPs) are most prominently investigated and their enhanced antibacterial, antiviral antioxidant effects have been extensively reported [4], [5]. AgNPs possess the unique properties like very high surface area, functionalizability and strong antimicrobial activity etc., due to which they find potential applications in several areas such as biomedicine, environmental remediation and electronics [6]. AgNPs have more bioactive properties compared to their bulk silver form, and, at the same time, make suitable candidates for drug or chemical agents delivery systems, wound treatment applications as well as additives in diverse consumer products [7].

Nanoparticles can be synthesized by different methodologies depending on the method used for the synthesis (conventional, chemical and physical and green synthesis) [8]. Common approaches based on chemical reduction (or physical processes, such as laser ablation or thermal evaporation) generally use toxic reagents and high-energy inputs to fabricate the desired NPs, leading to formation of hazardous by-products [9]. These limitations have opened the door for growing interest in the green synthesis where biological entities such as plant extracts, microorganisms and enzyme systems are employed to bioreduce metal ions into their nanoscale size [10]. Green syntheses are one of the most favored sustainable and green protocols compared with other methods, due to their relatively simplicity, low-cost, and less hazardous to health inorganic reagents. It further reduces the amount of unsafe materials to be used, and is a potential method for the preparation of NPs for medical and environmental remediation [11]. AgNPs are commonly synthesized using plant extracts, benefiting from the higher number of bioactive phytochemicals in plants that act as reducing agents and capping ligands for metal ions and NPs, respectively [12]. Hydrogels are widely recognized as excellent candidates for medical and environmental applications due to their biocompatibility, high water content, and ability to undergo easy modification [13] [14],[15] . Their versatile properties, such as responsiveness to environmental stimuli and controlled release capabilities, make them ideal for a variety of uses, including drug delivery systems and environmental remediation [16], [17], [18]. These characteristics also position hydrogels as promising materials for the synthesis and stabilization of nanoparticles (NPs), enhancing their potential in biomedical and environmental fields [19], [20], [21].

Chia (*Salvia hispanica* L.), a member of the mint family, is an annual herb plant growing in Central and South America, and exists with higher nutritional and health benefits [22], [23], [24]. Chia seeds are an excellent source of omega-3 fatty acids, protein, dietary fibre and antioxidants which is useful for human consumption [25], [26]. Plan extract contains phenolic compounds and flavonoids among other bioactive molecules act as reducing and capping agent of NPs [27].

The aim of this study is to explore the green synthesis of AgNPs using chia seed mucilage and evaluate their, *in vitro* antioxidant, antidiabetic, and anti-inflammatory activities. Chia seeds are chosen for their rich phytochemical profile, which may play a crucial role in enhancing the biological properties of the synthesized AgNPs. The current study focuses on optimizing the synthesis conditions, characterizing the AgNPs using various techniques such as UV-Vis spectroscopy, X-ray diffraction (XRD), scanning electron microscopy (SEM), and energy-dispersive X-ray spectroscopy (EDX), and assessing their biological activities. This study not only contributes to the development of sustainable nanomaterials but also opens new avenues for the use of plant-based synthesized nanoparticles in therapeutic application

## 2. Material and Methods

### 2.1 Extraction

Chia seed extracts were obtained by a simple aqueous extraction. Chia seeds were initially washed to remove impurities and dust. The homogeneous seeds sample (10 g) were then soaked in 100 mL of DW and allowed to stand for 24 h at room temperature, with then

stirrer at room temperature for 5 h, according to protocol developed by Assad et al., (2024) with minor modifications [28]. The clear mucilage was obtained, subsequently filter the soaked mixture through Whatman filter paper no 42. The filtrate was refrigerated (4°C) for further use.

**2.2 Biosynthesis of Silver Nanoparticles**

The AgNPs were biosynthesized by a 1 mM concentration of silver nitrate ($AgNO_3$) solution mixed with chia seeds extract at ratio 10:10 mL [29]. The mixture was then irradiated under direct sunlight for 5 min on a clear sunny day. Over a period, the reaction mixture was observed for color change since reduction of silver ions to metallic silver leads to formation of AgNPs, which manifested as colour change from pale yellow to brown or yellowish-brown. Finally, AgNPs were centrifuge at 1000 rpm for 10 min as depicted in Figure 1. The formation of AgNPs was confirmed by UV-Vis spectra of the solution after completion of the reaction. The biogenic AgNPs were named as SH@AgNPs and preserved for further studies and applications.

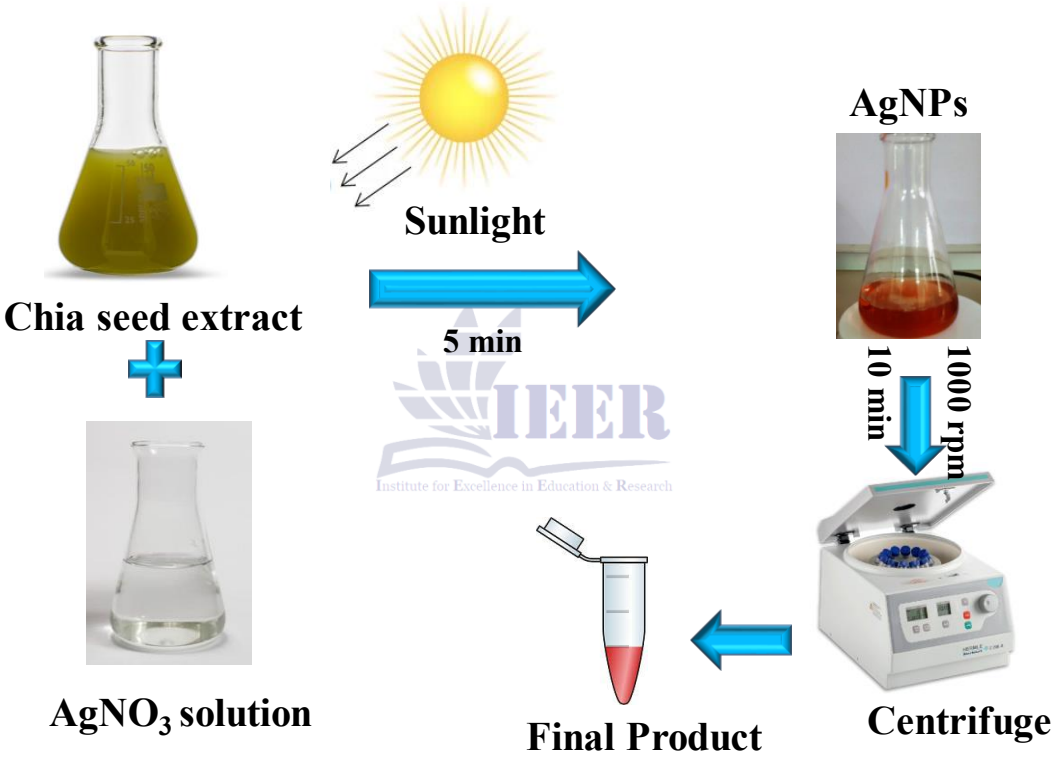


**Figure 1: Schematic representation of SH@AgNPs.**

**2.3 Characterization**

SH@AgNPs were extensively characterized using different analytical tools to determine their structural, optical and morphological features. The reduction of Ag ions was verified by UV-Vis spectroscopy ranging from 200 - 800 nm. X-ray diffraction (XRD) patterns confirmed the crystalline state of the SH@AgNPs, and scanning electron microscopy (SEM) provided insights into their dimensions and morphology. The existence of silver in the NPs and their composition were further identified by energy-dispersive X-ray spectroscopy (EDX). These characterizations were carried out to confirm the successful synthesis and quality of the SH@AgNPs for biological studies.

**2.4 Antioxidant Activity**

**2..4.1 DPPH Antioxidant Activity**

The antioxidant efficacy of the biosynthesized SH@AgNPs was determined by DPPH free radical scavenging method [30]. Stock solution of DPPH (0.1 mM) was diluted with methanol, the different concentrations (50–250 µg/mL) of SH@AgNPs were

mixed in methanol. One mLof each AgNP solution was mixed with 1 mL of DPPH solution, and then the mixture was kept in dark at room temperature for 30 min. Ascorbic acid was used as standard. The decrease in DPPH radical concentration was assayed through the determination of the absorbance at 517 nm with an UV-Vis spectrophotometer. The radical scavenging activities were expressed as a percentage according to the equation: Eq. 1:

$$\% \text{ RSA} = \left(\frac{Abs\ of\ control\ 517 - Abs\ of\ sample\ 517)}{Abs\ of\ control\ 517}\right) \times 100 \quad \text{(Eq. 1)}$$

**2.4.2 Ferric Reducing Antioxidant Power Activity**

The antioxidant potential of the biosynthesized SH@AgNPs was also evaluated through FRAP (Ferric Reducing Antioxidant Power) assay [31]. The FRAP reagent was prepared freshly by combining 10 mM of 2,4,6-tripyridyl-s-triazine (TPTZ) in HCl (40 mM), ferric chloride ($FeCl_3$) solution (20 mM), and acetate buffer adjusted to pH 3.6 at a ratio of 1:1:10). The reducing power was estimated by the addition of 1 mL different concentrations (50–250 µg/mL) SH@AgNPs and 2.5 mL FRAP reagent at 37 °C for incubation that continued for 30 min. The absorbance was read at 593 nm on a UV-Vis spectrophotometer. FRAP was determined by the comparison of absorbance of sample with standard calibration curve established from different concentrations ascorbic acid. The antioxidant capacity was reported as the FRAP value that represents its power to reduce ferric ions into ferrous ions, and the higher value of FRAP indicates a stronger reducing capability. FRAP activity was calculated using the Eq. 2.

$$X = \left(\frac{y)}{0.0026}\right) R2 = 0.99 \quad \text{(Eq. 2)}$$

**2.5 *In vitro* Antidiabetic Activity**

**2.5.1 Starch Hydrolysis**

The ability of the biosynthesized chia seed mucialge mediated AgNPs to inhibit starch hydrolysis was assessed using a previously reported α-amylase inhibition assay developed by (Assad et al., 2025) with minor modifications [32]. Agar plates were prepared using a nutritive matrix supplemented with soluble starch (1% w/v). Once solidified, three uniform wells were made in each plate. An α-amylase preparation from *Aspergillus oryzae* (2 U/mL) in phosphate buffer (pH 6.9) served as the positive hydrolysis control and was dispensed into well A, Well B: Standard inhibitor acarbose (20 µg/mL) and α-amylase and Well C: Green-synthesized AgNPs (20 µg/mL) and α-amylase. For 30 µg/mL, in Well B: Standard inhibitor acarbose (30 µg/mL) and α-amylase and Well C: Green-synthesized AgNPs (30 µg/mL) and α-amylase. The inoculated plates were incubated under controlled conditions to allow enzymatic interaction with the starch substrate for 48 h. After the incubation period, the agar surfaces were treated with an iodine–potassium iodide solution (0.5 mM $I_2$ in 3% KI). Iodine staining enabled visualization of starch-rich areas, while clear halos surrounding each well indicated zones, where starch had been hydrolyzed. The diameter of each clear zone (mm) was measured, and the inhibitory effect of the AgNPs was quantified by comparing the hydrolysis zone produced by AgNPs with that of the α-amylase control. Results were expressed as percentage inhibition using the following Eq.3.

$$\% \ \alpha - \text{amylase inhibition} = \left(\frac{diameter\ of\ control\ -\ diameter\ of\ sample)}{diameter\ of\ the\ control}\right) \times 100 \quad \text{(Eq. 3)}$$

**2.5.2 Enzyme Kinetics Study**

The α-amylase inhibitory activity of the biosynthesized AgNPs was evaluated following a previously established method with minor modifications [32]. Briefly, different concentrations of the SH@AgNPs (10–30 µg/mL) were prepared and incubated with α-amylase prepared in phosphate buffer (pH 6.9). After a short pre-incubation period, soluble starch was added as the substrate and the reaction mixture was further incubated under controlled temperature conditions to allow enzymatic hydrolysis. The reaction was terminated using a color-developing DNS reagent, followed by heat treatment to permit chromophore formation. After cooling, the mixtures were diluted appropriately and the absorbance was measured at 540 nm. The degree of α-amylase inhibition by the AgNPs was quantified by comparing the absorbance of SH@AgNPs treated samples with that of the

negative control. The percentage inhibition was calculated using the standard equation based on the reduction in absorbance relative to the untreated control (Eq.4).

$$\% \text{ inhibition} = \left(\frac{K - S)}{K}\right) \times 100 \quad (Eq. 4)$$

K=Absorption of negative controls; S=Absorbance of sample/Absorbance of positive control.

### 2.6 Anti-inflammatory Activity

*In vitro* anti-inflammatory activity of the AgNPs was studied by screening protein denaturation, employing egg albumin as a standard[33]. In this method, different concentration of AgNPs 50-250 µg/mL were added to the solutions of protein which is prepared from fresh egg albumin solution under controlled pH. The resulting mixtures were heat-induced denatured by controlled exposure to a temperature where albumin proteins normally undergo conformational changes leading to an increase in turbidity. Absorbance of each solution was read after the heating process followed by cooling and consequently comparison with the untreated control helped in assessing the degree of protein denaturation. Diclofenac sodium was used as standard anti-inflammatory drug and reference control for comparison. The % inhibition of protein denaturation was determined using the following Eq. 5.

$$Inhibition\ of\ protein\ denaturation\ (\%) = \left(1 - \frac{\text{Absorbance of sample}}{\text{Absorbance control}}\right) \times 100 \quad (\text{Eq. } 5)$$

### 2.7 Statistical analysis

All the experiments were carried out in triplicate, expressed as mean ± SD. The raw experimental data were collected and summarized with Microsoft Word 2016 (Microsoft) and Excel, initially. Dose–response curves and comparative analyses were prepared using Origin 2021 software.

## 3. Results and Discussion

### 3.1 Optical Analysis

In the present study, the UV–Visible absorption spectrum of the biosynthesized SH@AgNPs exhibited well-defined surface-plasmon-resonance (SPR) band at 426nm (Figure 2), which is in good agreement with typical wavelength for spherical AgNPs synthsized through green approaches as reported (400–450nm). The SPR bands are attributed to the collective oscillations of conduction electrons on NP surfaces due to incident light, and their existence is generally considered as conclusive proof for the formation of metallic AgNPs [34]. In an earlier study, Liaqat et al. (2022) reported the absorption maxima for the AgNPs prepared via plant extract were recorded at 425 nm which also supports that our findings reflect successful NPs formation and small particle size [35]. Moreover, the position and shape of the SPR peak also provide information about size, information and degree of aggregation on the NPs: a small red shifted or broader peak is generally associated to larger particle size or some amount of agglomerations [36]. In this study SPR band at 426 nm indicates the good colloidal stability and narrow size distribution that emphasizes towards relatively small uniform NPs in agreement with the recent study on green synthesized AgNPs, wherein SPR maxima was recorded around 420 nm [37]. Therefore, the UV–Vis analysis validates the formation of crystalline AgNPs, and supports further investigations of their biological activity.

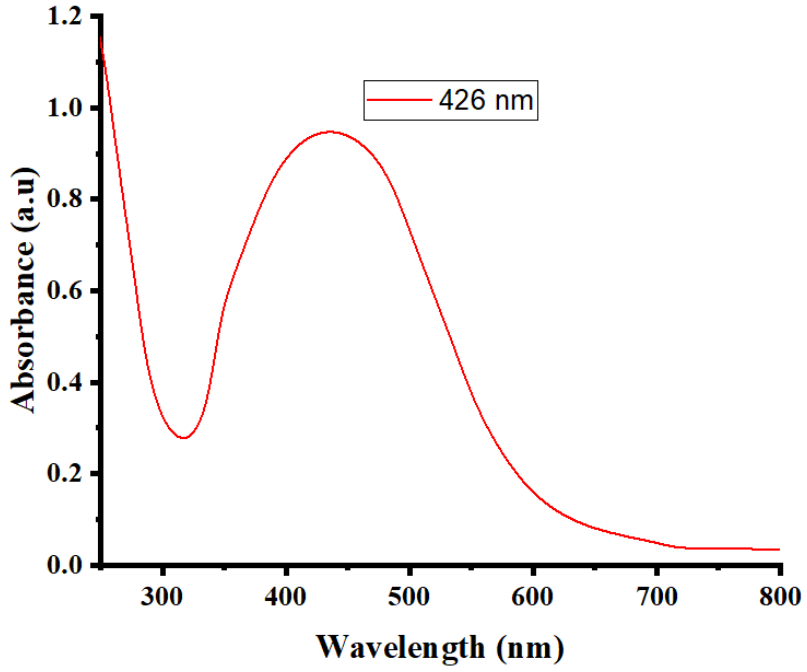


**Figure 2: UV-Visible absorption spectrum of biosynthesized SH@AgNPs.**

### 3.2 XRD Analysis

The XRD spectrum of biosynthesized SH@AgNPs showed characteristic peaks at 2θ = 38°, 44°, 64° and 77° which were indexed to the crystallographic planes (111), (200), (220) and (311)m respectively as depicted in Figure 3. These peaks are assigned to face-centered cubic (FCC) structure of AgNPs, which is in agreement with known crystal structure of metallic AgNPs [38]. The sharpness and strong intensity of these peaks further reveal that the biosynthesized SH@AgNPs are highly crystalline revealing the formation of NPs with well arrangement. This finding is consistent with those from Asif et al. (2022) who also observed similar diffraction peaks for green synthesized AgNPs, confirming their crystallinity and purity [39].

The appearance of these characteristic peaks confirms the formation AgNPs that have dominant FCC structure, and also noticed a few peaks marked with (*) corresponding to plant extracts as a reducing and capping agent [40]. The lack of additional peaks related to secondary phases also confirms that the synthesized AgNPs are phase pure, without any contamination from other silver compounds or impurities.

The XRD pattern provides valuable understanding into the size and morphology of the synthesized AgNPs. The narrowness of the diffraction peaks indicates relatively small, well-dispersed NPs suitable for biomedical and environmental application. The small broadening of these peaks may indicate the presence of nanoscale particles with sizes typically ranging from 10 to 100 nm, as noted in previous reports of green-synthesized AgNPs [41], [29].

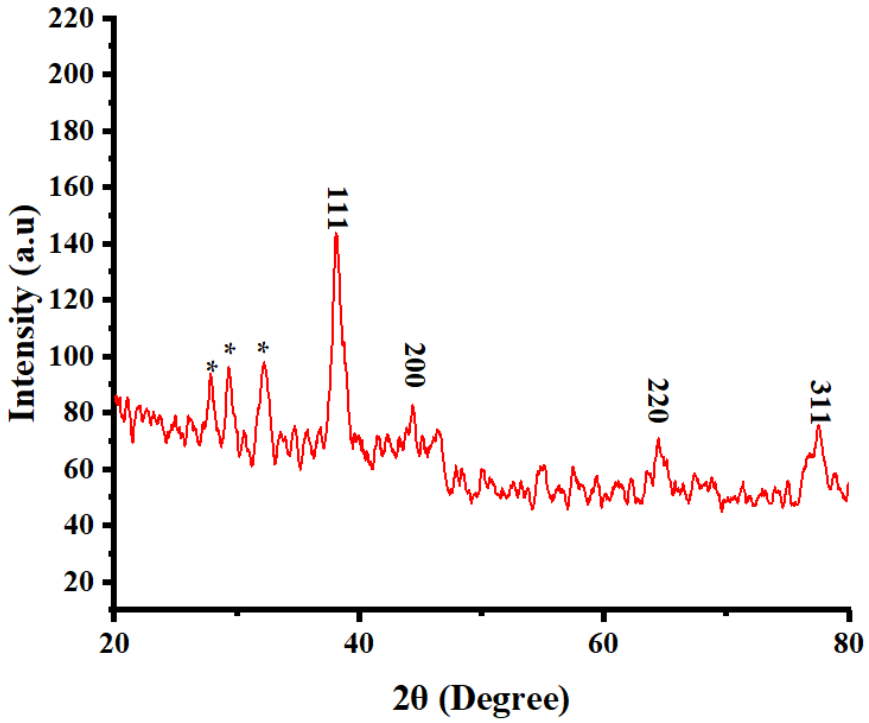


**Figure 3: X-ray diffraction (XRD) pattern of the biosynthesized AgNPs.**

### 3.3 SEM Analysis

The morphology of the green synthesized SH@AgNPs was investigated by SEM. In the low-magnification image (Figure 4 A), NPs present as aggregated clumps with rough contours, which is typical in plant mediated synthesis of NPs, where biomolecules are the reducers and the capping agents leading to mild agglomeration [42]. At a high magnification (Figure 4 B) SH @AgNPs exhibit a mostly round particle shape and homogenest size distribution which indicates great capacity of the biological synthesis route to control particle shape and growth. The histogram of the particle size distribution (Figure 4 C) gives an average diameter of 82.02±2.7nm, with most particles falling in the range from 75 to 90 nm. The small size distribution and well-ordered morphology are in good agreement with previous study [43]. The SEM findings confirm that the synthesized AgNPs are relatively well controlled in size and shape.

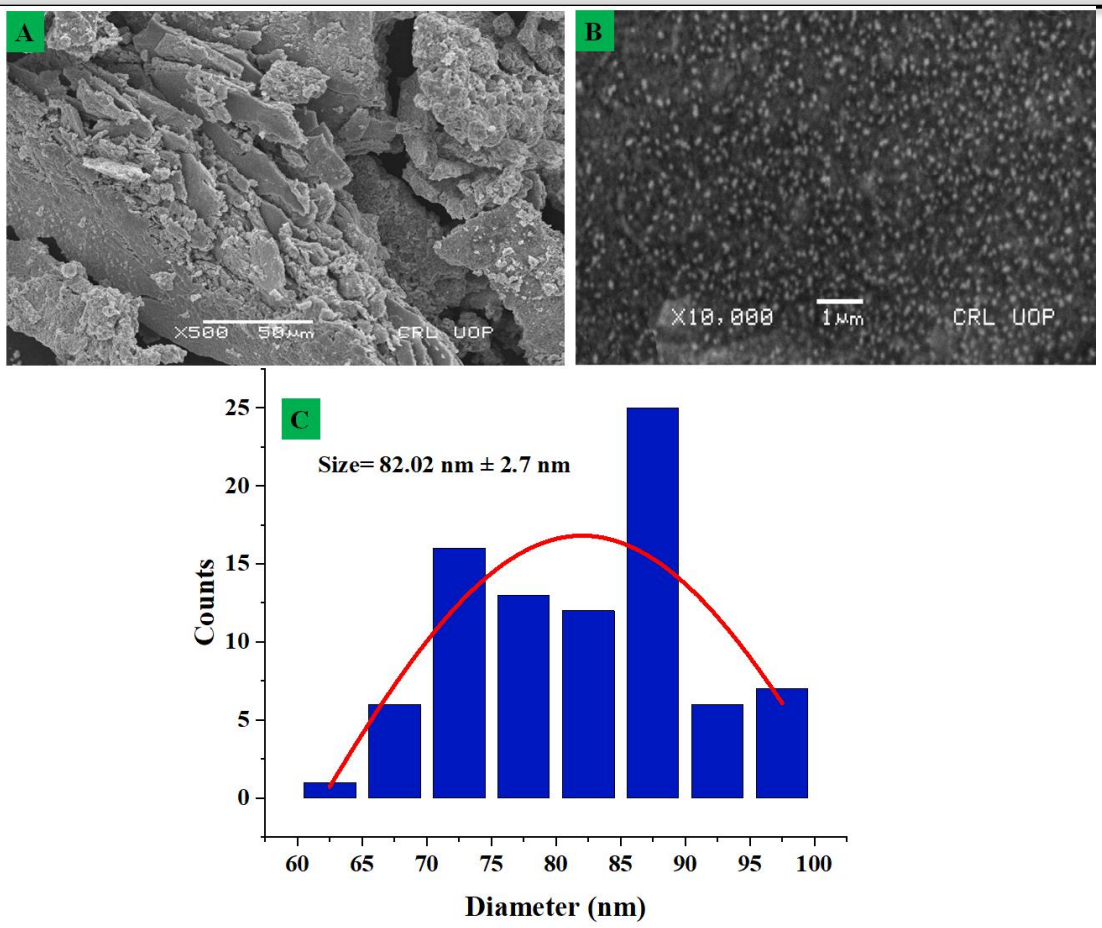




Figure 5. The SEM image of the biosynthesized AgNPs. (A) at low magnification (×500) and indicates aggregate irregular shaped particles. (B) at high-magnification image (×10,000) of the NPs mainly spherical and evenly distributed. (C) shows the particle size distribution histogram.

### 3.4 EDX Analysis

The elemental components of SH@AgNPs were further confirmed by energy-dispersive X-ray spectroscopy (EDX). The typical peaks of the characteristic X-ray emission of silver that is the main component in the biosynthesized SH@AgNPs can be observed from EDX spectrum (Figure 5). The peak around 3 keV is associated with the Lα transition of silver which proves the existence of AgNPs [44], [33]. Besides silver, carbon (C), oxygen (O), sodium (Na), silicon (Si), and chlorine (Cl) are identified from the elemental peaks in the spectrum. These may be attributed to the mucilage and sample preparation. The carbon and oxygen in particular, could be associated to organic moieties of the plant extract that participate in the reduction as well as capping of the AgNPs [45]. The wt. % of Ag was 60.08 %, which shows that silver is the main component in NPs. The content of Ag atomic percentage was computed to be 28.78%, indicating that the sample is mainly contributed by silver [46]. These results demonstrate the successful synthesis of SH@AgNPs.

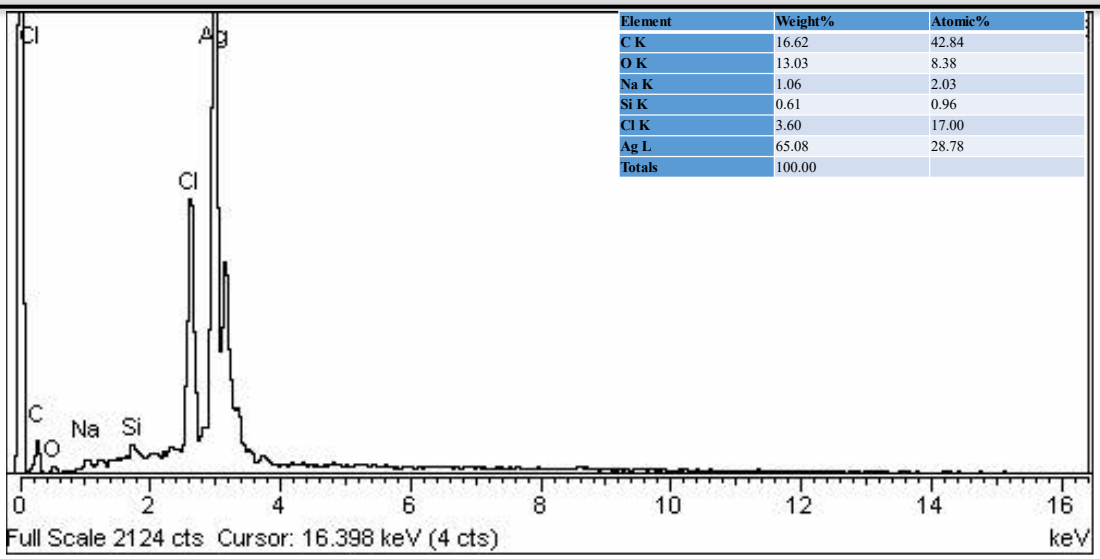


| Element | Weight% | Atomic% |
|---|---|---|
| C K | 16.62 | 42.84 |
| O K | 13.03 | 8.38 |
| Na K | 1.06 | 2.03 |
| Si K | 0.61 | 0.96 |
| Cl K | 3.60 | 17.00 |
| Ag L | 65.08 | 28.78 |
| Totals | 100.00 | |

**Figure 5: EDX analysis of biosynthesized SH@AgNPs.**

### 3.5 Antioxidant Activity of SH@AgNPs

#### 3.5.1 DPPH Assay for Antioxidant Activity of SH@AgNPs

The antioxidant potential of the synthesized SH@AgNPs was determined by the measurement of the DPPH (2, 2-diphenyl-1-picrylhydrazyl) radical scavenging activity, a frequently used method for examining an electron donating capacity and free radical quenching potential. Data are expressed in percentage of inhibition of DPPH radical and the activity was compared to ascorbic acid (AA), standard antioxidant.

In Figure 6, the antioxidant activity of both SH@AgNPs and AA was dose-dependent when the concentration ranged from 100 µg/mL to 500 µg/mL. The SH@AgNPs was inhibited by 41.09 % at the concentration of 100 µg/mL, which is lower than that of ascorbic acid (44.81%). SH@AgNPs demonstrated 67.24% inhibition at the highest concentration of 500 µg/mL, whereas ascorbic acid displayed 72.31%. This suggests that SH@AgNPs presented strong and good antioxidant performance, especially with the increase of concentration. The results show that the green synthesized of SH@AgNPs have moderate antioxidant in comparison to ascorbic acid which used as a common antioxidant.

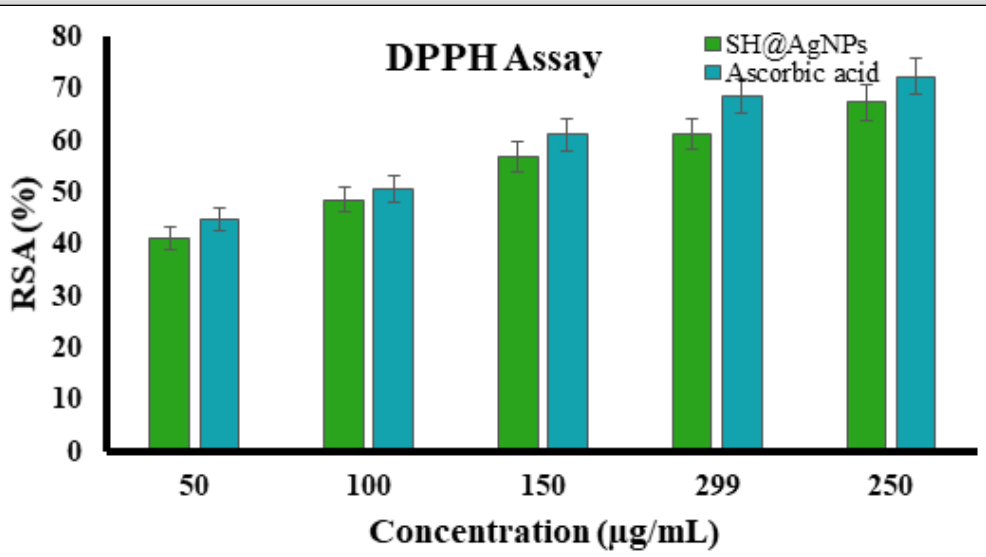


**Figure 6: Radical scavenging activity of SH@AgNPs and ascorbic acid was analyzed using DPPH.**

### 3.5.2 FRAP Assay for Antioxidant Activity of SH@AgNPs

The antioxidant capacity of the biosynthesized SH@AgNPs was tested utilizing FRAP, which is based on providing a measure of the sample's ability to reduce $Fe^{3+}$ ions to $Fe^{2+}$. The data are expressed in AAE (Ascorbic Acid Equivalent) values and a higher the latter value means stronger antioxidant activity.

As presented in Figure 7, both SH@AgNPs and ascorbic acid showed a concentration-dependent enhancement in antioxidant activity. At 250 µg/mL, SH@AgNPs produced an inhibition of 63.59 µg/mL AAE, comparable to that elicited by ascorbic acid (68.25 µg/mL AAE). At 100 µg/mL, SH@AgNPs recorded the maximum inhibition capacity (32.85 µg/mL AAE) when compared to ascorbic acid which exhibited an inhibition of 38.54 µg/ mL AAE. This comparison reveals that SH@AgNPs have a strong antioxidant activity, at slightly low level from the corresponding concentration of ascorbic acid. The data indicate that the green synthesis approach with chia seed mucilage (as natural reducing agent) efficiently stabilized the AgNPs and also increased their potential as antioxidant agents.

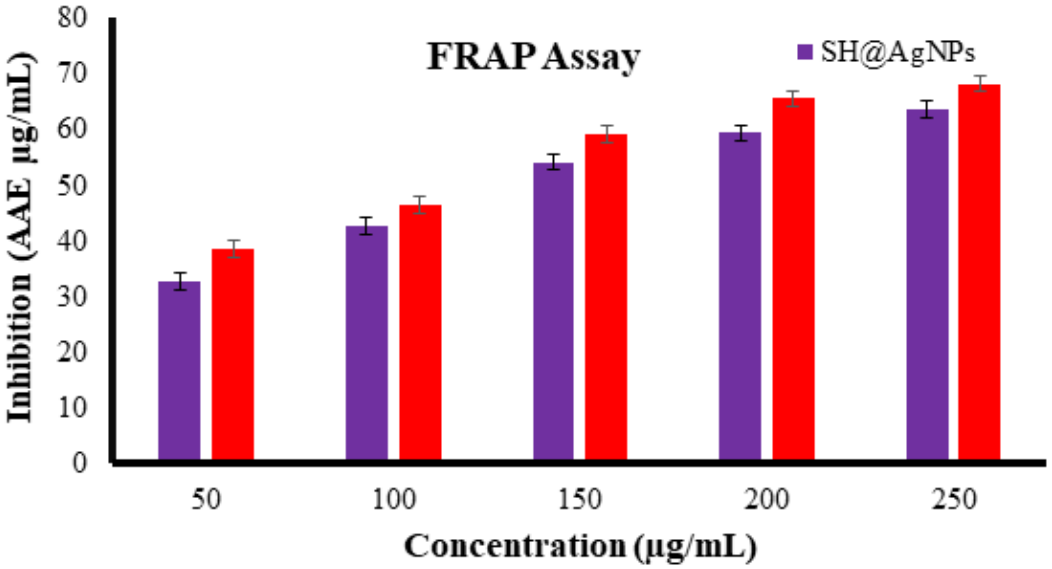


**Figure 7: FRAP assay estimation of the antioxidant activity of SH@AgNPs and ascorbic acid.**

### 3.6 *In vitro* Antidiabetic of SH@AgNPs

#### 3.6.1 Starch Hydrolysis

Diabetes mellitus is a chronic metabolic disease caused by defective insulin secretion or action that results in elevated blood glucose (hyperglycemia) [47]. The two most common types are Type 1 diabetes, in which the pancreas doesn't produce insulin and an autoimmune condition causes the body to destroy it, and Type 2 diabetes, in which the body resists insulin or is unable to use it effectively [48]. The accelerating rates of diabetes across the globe becomes a major public health issue considering that co-morbidities associated with this disease include cardiovascular diseases, neuropathy, renal failure and vision loss. Treatment usually consists of dietary changes, oral medications and sometimes insulin. Given this, there is an increased interest in natural and alternative therapies such as the use of enzyme inhibitors, which may potentially control blood glucose level and disease better [49].

The starch-hydrolysing inhibition potential of the synthesized SH@AgNPs was evaluated using a zone of hydrolysis assay on agar plates with Acarbose as the standard inhibitor [22]. Acarbose had an 18mm zone (58.57% inhibition) at 20µg/mL and a 15mm zone (60.00% inhibition) at 30µg/mL. The SH@AgNPs showed 20mm (31.42% inhibition) at 20µg/mL and 18mm (45.71% inhibition) at 30µg/mL, which indicated a dose dependent increase in zone of inhibition (Table 1). These findings are also in agreement with earlier literature reports on the capacity of green-synthesized AgNPs to inhibit carbohydrate-digesting enzymes [50]. Similarly, NPs synthesized from *Azadirachta indica* also showed α-amylase inhibitory activity with evident dose-dependent [51]. Additionally, while the AgNPs of *Pleurotus giganteus* are also able to inhibit α-amylase and has been identified as a reversible non-competitive inhibitor [52]. The comparatively lower inhibition shown by SH@AgNPs compared to Acarbose may reflect differences in nanoparticle size, capping biomolecules, enzyme–nanoparticle interaction kinetics, or dispersion effects. Importantly, the SH@AgNPs values still fall within the range of inhibitory activity reported for similar green-synthesized AgNPs, supporting their potential utility as antidiabetic agents via modulation of starch digestion. In this context, the inhibition of α-amylase helps delay starch-to-glucose conversion and reduce post-prandial hyperglycaemia [53]. Thus, the present results add to the increasing evidence that green synthesized AgNPs could act as effective enzyme-inhibitors for metabolic diseases.



**Table 1: Inhibition of starch hydrolysis by Acarbose and SH@AgNPs at different concentrations**

| Solution | Concentration (µg/mL) | Zone of Inhibition (mm) | % Inhibition |
|---|---|---|---|
| Standard (Acarbose) | 20 | 18 | 58.57 |
| | 30 | 15 | 60.00 |
| SH@AgNPs | 20 | 20 | 31.42 |
| | 30 | 18 | 45.7 |

#### 3.6.2 Enzyme Kinetics

The enzyme kinetics of the biosynthesized SH@AgNPs were evaluated using the α-amylase inhibition assay based on the dinitrosalicylic acid (DNSA) method. The percentage inhibition of α-amylase activity was calculated from the reduction in absorbance of the reaction mixture at 540 nm. The data indicate a dose-dependent increase in α-amylase inhibition with higher concentrations of SH@AgNPs, as shown in Figure (8A and B).

These findings indicate a notable dose-dependent inhibition of α-amylase activity by SH@AgNPs, possibly exerting an antidiabetic impact. The concentration-dependent inhibition showed that NPs might bind to the active site of the enzyme or its interaction with the enzyme-substrate complex was

disturbed, decreasing hydrolysis process for starch [33], [32].

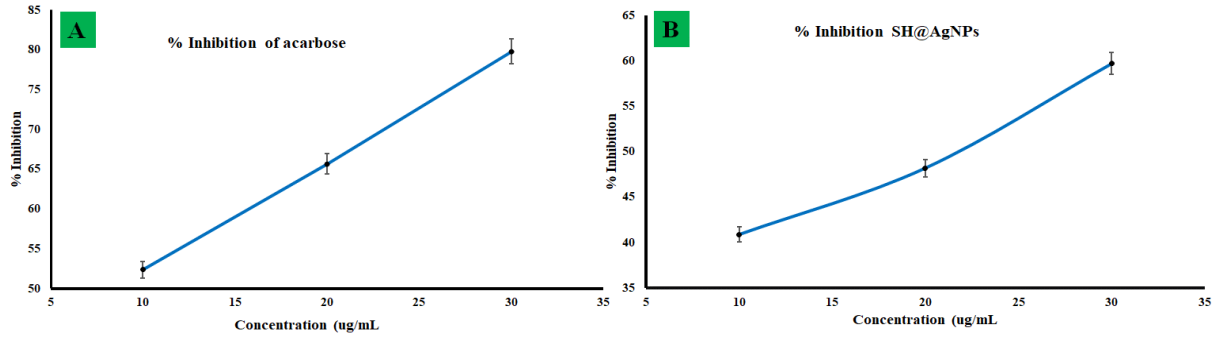


**Figure 8: Dose-dependent inhibition of α-amylase by Acarbose (A) and (B) SH@AgNPs at various concentrations 10, 20 and 30 µg/mL.**

### 3.7 Anti-inflammatory Activity of SH@AgNPs

The anti-inflammatory activity of the biosynthesized SH@AgNPs was assessed *in vitro* using a standard model of protein denaturation. The AgNPs exhibited a clear dose-dependent inhibition: at 50 µg/mL they showed approximately 44.00 % inhibition, which increased progressively to 78.56 % inhibition at 250 µg/mL. While the reference drug, diclofenac sodium (500 µg/mL), achieved 83.18% inhibition under the same conditions, the results indicate that SH@AgNPs possess substantial anti-inflammatory potential, approaching that of a standard pharmaceutical agent as shown in Table 2. This behavior aligns with earlier studies where green synthesized AgNPs demonstrated significant anti-inflammatory effects; for example, Singh et al. reported effective inhibition of inflammatory responses by spherical AgNPs synthesized from *Pyrus serrulata* extract. Similarly, green synthesized AgNPs from *Nephthea* sp. were shown to inhibit both COX-1 and COX-2 enzymes at low microgram concentrations. Moreover, Diallo et al. used *Aphania senegalensis* leaf extract to synthesize AgNPs that exhibited notable anti-inflammatory activity *in vitro*, further supporting the potential of plant-mediated AgNPs in inflammation management [54]. These findings suggest the SH@AgNPs can serve as promising candidates for further *in vivo* and mechanistic anti-inflammatory investigations.

Anti-inflammatory activity of the bio-fabricated SH@AgNPs was evaluated in vitro, against a model protein denaturation system. The inhibition of AgNPs was observed to be dose-dependent: at 50µg/mL 44.00 %, at 250µg/mL 78.56 % were observed. Under similar conditions, the reference drug, diclofenac sodium (500 µg/mL) exerted 83.18 % inhibition, and these results suggest that SH@AgNPs have strong anti-inflammatory effects that are comparable to those of a standard as shown in Table 2. These behaviors were consistent with previous investigations where green mediated AgNPs showed strong anti-inflammatory activities. Singh et al., (2017) studied successful suppression of inflammatory responses using spherical AgNPs prepared with *Pyrus serrulata* extract [55]. Similarly, biofabricated AgNPs of *Nephthea* sp. were demonstrated to inhibit the activity of COX-1 and COX-2 enzymes at low concentrations [56]. Moreover, Diallo et al., (2024) formulated AgNPs using leaf extract of *Aphania senegalensis* and the synthesized demonstrated significant *in vitro* anti-inflammatory effect, consolidating the therapeutic potential of plant bio mediated AgNPs in inflammation healing (Diallo et al., 2024). The, results demonstrate that the SH@AgNPs may be considered as potential candidates for future *in vivo* and mechanistic anti-inflammatory studies.

Table 2. Anti-inflammatory activity of SH@AgNPs and Diclofenac sodium at varying concentrations.

| Concentration (µg mL$^{-1}$) | SH@AgNPs (% Inhibition) | Diclofenac sodium (500 µg mL$^{-1}$) (% Inhibition) |
|---|---|---|
| 50 | 44.00 | |
| 100 | 55.50 | |
| 150 | 63.73 | 83.18 |
| 200 | 72.84 | |
| 250 | 78.56 | |

## 4. Conclusion

The present investigation demonstrated the successful synthesis of silver nanoparticles (SH@AgNPs) by green route using chia (*Salvia hispanica* L.) seed mucilage. The nanoparticles were characterized by UV-Vis spectroscopy and showed a well-defined surface plasmon resonance (SPR) at 426 nm indicating the formation of AgNPs. The crystalline nature of the as-synthesized nanoparticles were determined by X-ray diffraction (XRD), peaks indicating that particles possessed a face-centered cubic (FCC) structure of silver. Scanning electron microscopy (SEM) micrographs revealed that the nanoparticles were spherical in shape and 82.02 ± 2.7 nm, thus a narrow size distribution was obtained for each particle. These analyses were also confirmed by energy-dispersive X-ray spectroscopy (EDX) which showed silver in the nanoparticles for further confirmation of their composition. *In vitro* biological effects of SH@AgNPs, including potent antioxidant, antidiabetic, and anti-inflammatory activities were observed. SH@AgNPs possessed remarkable DPPH and FRAP scavenging activities even at lower concentration. The α-amylase inhibitory activity was dose-dependent and hydrolysis of starch was inhibited at a maximal rate of 45.71% at 30 µg/mL. Enzyme kinetics investigations also supported the antidiabetic activity of SH@AgNPs. The anti-inflammatory potential of SH@AgNPs was evaluated against egg albumin denaturation model and the inhibition percentage was found to be 78.56% which is almost equivalent with that demonstrated by Diclofenac sodium. The findings suggest versatile application of SH@AgNPs in antioxidant, antidiabetic, and anti-inflammatory treatments. The green synthesis method not only offers an ecofriendly and sustainable path but also produce nanoparticles with excellent biocompatibility that makes them to be future potential candidates for other biomedical applications as well as therapeutic usage.

## 5. REFERENCES

1. Tawiah, B., Ofori, E. A. & George, S. C. Nanotechnology in societal development. in *nanotechnology in societal development* (eds George, S. C. & Tawiah, B.) 1–64 (Springer Nature Singapore, Singapore, 2024). doi:10.1007/978-981-97-6184-5_1.
2. Kanwal, M. *et al.* Dual colorimetric sensing of Hg (II) and Fe (III) using sulfanilamide-stabilized silver nanoparticles and evaluating their photodegradation and antibacterial properties. *Journal of Water Process Engineering* **75**, 107981 (2025).
3. Ghaffar, S. *et al.* Improved photocatalytic and antioxidant activity of olive fruit extract-mediated ZnO nanoparticles. *Antioxidants* **12**, 1201 (2023).
4. Hashmi, S. S. *et al.* Green synthesis of silver nanoparticles from *Olea europaea* L. extracted polysaccharides, characterization, and its assessment as an antimicrobial agent against multiple pathogenic microbes. *Open Chemistry* **22**, 20240016 (2024).
5. Roheen, T. *et al.* enhanced antibacterial and anti-inflammatory efficiency of serratiopeptidase immobilized on CMC-silver nanoparticles. *Journal of Basic Microbiology* **65**, e70060 (2025).
6. Bamal, D. *et al.* Silver nanoparticles biosynthesis, characterization, antimicrobial activities, applications, cytotoxicity and safety issues: An updated review. *Nanomaterials* **11**, 2086 (2021).
7. Huq, M. A. *et al.* Green synthesis and potential antibacterial applications of bioactive silver nanoparticles: A review. *Polymers* **14**, 742 (2022).

8. Assad, N. *et al.* Nanotechnology in oilseed crops: a new frontier for abiotic stress adaptation. in *oilseed crops under abiotic stress* (ed. Abdel Latef, A. A. H.) 507–536 (Springer Nature Singapore, Singapore, 2025). doi:10.1007/978-981-96-8346-8_16.
9. Triphati, A. & Pirzadah, T. B. Synthesis methods of nanoparticles and their key applications. in *Synthesis of Bionanomaterials for Biomedical Applications* 57–76 (Elsevier, 2023).
10. Gula, H. *et al.* Exploring the antibacterial, anticoagulant, and hemolytic potential of green-synthesized $Fe_2O_3$ Nanoparticles by *Cucurbita pepo* pulp. *IEEE Transactions on NanoBioscience* https://ieeexplore.ieee.org/abstract/document/10973190/ (2025).
11. Madani, M. *et al.* Green synthesis of nanoparticles for varied applications: Green renewable resources and energy-efficient synthetic routes. *Nanotechnology Reviews* **11**, 731–759 (2022).
12. Shaikh, W. A. *et al.* A review of the phytochemical mediated synthesis of AgNP (silver nanoparticle): the wonder particle of the past decade. *Appl Nanosci* **11**, 2625–2660 (2021).
13. Khatoon, M. *et al.* A chia (*Salvia hispanica* L.) seed mucilage-based glucoxylan-grafted-acrylic acid hydrogel: a smart material for pH-responsive drug delivery systems. *Materials Advances* **6**, 2636–2647 (2025).
14. Bukhari, S. N. A. *et al.* Extraction optimization of mucilage from seeds of *Mimosa pudica* by response surface methodology. *Polymers* **14**, 1904 (2022).
15. Hussain, M. A. *et al.* Cross-linking of hydroxypropylcellulose with flaxseed rhamnogalacturonans using citric acid produces a hemocompatible biocomposite for pH - responsive rifaximin delivery. *Journal of Applied Polymer Science*, **142**, e57486 (2025).
16. Hussain, M. A. *et al.* Removal of Cr (III) and Ni (II) from aqueous solution using a mixed cellulose ether-ester hydroxyethylcellulose adipate. *Desalination and Water Treatment* **283**, 153–163 (2023).
17. Hussain, M. A. *et al.* Adsorptive removal of $Pb^{2+}$ and $Cu^{2+}$ from aqueous solution using an acid modified glucuronoxylan-based adsorbent. *Desalination and Water Treatment* **248**, 163–175 (2022).
18. Hussain, M. A. *et al.* Optimization of rhamnogalacturonan extraction from linseed using RSM and designing a pH-responsive tablet formulation for sustained release of ciprofloxacin. *Cellulose Chemistry and Technology* **59**, 547–558 (2025).
19. Iqbal, J. *et al.* β-Cyclodextrin-functionalized silver nanoparticles as a visual probe for selective tetrahydrocannabinol detection via host–guest induced plasmonic shifts. *Microchemical Journal* 116177 (2025).
20. Fatima, A. *et al.* Acute oral toxicity evaluation of a copolymerized *Mimosa pudica* seed mucilage on rabbit as model animal. *Frontier in Medical and Health Research* **3**, 412–420 (2025).
21. Ali, A. *et al.* A model batch and column study for Cd (II) uptake using citric acid cross-linked *Salvia spinosa* hydrogel: optimization through Box-Behnken design. *Journal of Industrial and Engineering Chemistry*, 151, 746-761 (2025).
22. Zare, T., Fournier-Level, A., Ebert, B. & Roessner, U. Chia (*Salvia hispanica* L.), a functional 'superfood': new insights into its botanical, genetic and nutraceutical characteristics. *Annals of Botany* **134**, 725–746 (2024).
23. Ali, A. *et al.* A pH-responsive, biocompatible, and non-toxic citric acid cross-linked polysaccharide-based hydrogel from *Salvia spinosa* L. offering zero-order drug release. *Journal of Drug Delivery Science and Technology* **69**, 103144 (2022).
24. Ali, A. *et al.* A Smart hydrogel from *Salvia spinosa* seeds: pH responsiveness, On-off switching, sustained drug release, and transit detection. *Current Drug Delivery* **20**, 292–305 (2023).
25. Agarwal, A. *et al.* Nutritional and functional new perspectives and potential health benefits of quinoa and chia seeds. *Antioxidants* **12**, 1413 (2023).

26. Ali, A. *et al.* Synthesis, characterization, and acute toxicity of pH-responsive *Salvia spinosa* mucilage-co-acrylic acid hydrogel: A smart excipient for drug release applications. *Reactive and Functional Polymers* **182**, 105466 (2023).
27. Khatoon, M. *et al.* A superporous and pH-sensitive hydrogel from *Salvia hispanica* (chia) seeds: stimuli responsiveness, on–off switching, and pharmaceutical applications. *RSC Advances* **14**, 27764–27776 (2024).
28. Assad, N. *et al.* Photo-catalytic and biological applications of phyto-functionalized zinc oxide nanoparticles synthesized using a polar extract of Equisetum diffusum D. *RSC Advances* **14**, 22344–22358 (2024).
29. Assad, N. *et al.* Diffused sunlight assisted green synthesis of silver nanoparticles using *Cotoneaster nummularia* polar extract for antimicrobial and wound healing applications. *Natural Product Research* **39**, 2203–2217 (2025).
30. Noor, A. *et al.* Green synthesis of silver-doped ZnO nanoparticles from *Adiantum venustum* D. Don (Pteridaceae): antimicrobial and antioxidant evaluation. *Journal of Basic Microbiology* **65**, e2400543 (2025).
31. Hussain, S. B. *et al.* Characterization and comparative antibacterial activities of gold nanoparticles synthesized by *TAGETES PATULA* L. (Asteraceae) flower extract. *Microscopy Res & Technique* **88**, 1869–1880 (2025).
32. Assad, N. *et al.* Eco-friendly synthesis of gold nanoparticles using *Equisetum diffusum* D. Don. with broad-spectrum antibacterial, anticancer, antidiabetic, and antioxidant potentials. *Scientific Reports* **15**, 19246 (2025).
33. Khan, Z. U. R. *et al.* Aconitum lycoctonum L. (Ranunculaceae) mediated biogenic synthesis of silver nanoparticles as potential antioxidant, anti-inflammatory, antimicrobial and antidiabetic agents. *BMC Chemistry* **17**, 128 (2023).
34. Mukaratirwa-Muchanyereyi, N. *et al.* Synthesis of silver nanoparticles using plant extracts from Erythrina abyssinica aerial parts and assessment of their anti-bacterial and anti-oxidant activities. *Results in Chemistry* **4**, 100402 (2022).
35. Liaqat, N. *et al.* Green synthesized silver nanoparticles: Optimization, characterization, antimicrobial activity, and cytotoxicity study by hemolysis assay. *Frontiers in chemistry* **10**, 952006 (2022).
36. Ramzan, M. *et al.* Green synthesis and characterization of silver nanoparticles using *Zingiber officinale* extracts to investigate their antibacterial potential. *IJN* **Volume 19**, 13319–13338 (2024).
37. Sati, A. *et al.* Silver nanoparticles (AgNPs): comprehensive insights into bio/synthesis, key influencing factors, multifaceted applications, and toxicity-A 2024 Update. *ACS Omega* **10**, 7549–7582 (2025).
38. Fahim, M. *et al.* Green synthesis of silver nanoparticles: A comprehensive review of methods, influencing factors, and applications. *JCIS Open* **16**, 100125 (2024).
39. Asif, M. *et al.* Green synthesis of silver nanoparticles (AgNPs), structural characterization, and their antibacterial potential. *Dose-Response* **20**, 15593258221088709 (2022).
40. Hussain, M. A. *et al.* Development of a novel smart bio-composite hydrogel based on dextran, citric acid, and glucoxylan for pH-dependent drug delivery and stimuli-responsive swelling and release. *Polymers and Polymer Composites*, 33, 09673911251350240 (2025).
41. Jabbar, A. *et al.* A highly selective $Hg^{2+}$ colorimetric sensor and antimicrobial agent based on green synthesized silver nanoparticles using Equisetum diffusum extract. *RSC advances* **13**, 28666–28675 (2023).
42. Perugu, S. *et al.* Green synthesis of silver nanoparticles using leaf extract of medicinally potent plant *Saraca indica*: a novel study. *Appl Nanosci* **6**, 747–753 (2016).
43. Eker, F. *et al.* Green synthesis of silver nanoparticles using plant extracts: A comprehensive review of physicochemical properties and multifunctional applications. *International Journal of Molecular Sciences* **26**, 6222 (2025).

44. Datta, A. S. *et al.* Role of medicinal plant in synthesis of green silver nanoparticles as antibacterial agent. *Journal of Pharmacognosy and Phytochemistry* **13**, 318–325 (2024).
45. Pandey, P. *et al.* Biosynthesis of silver nanoparticles from plant extracts: a comprehensive review focused on anticancer therapy. *Frontiers in Pharmacology* **16**, 1600347 (2025).
46. Akhter, M. S. *et al.* A systematic review on green synthesis of silver nanoparticles using plants extract and their bio-medical applications. *Heliyon* **10**, (2024).
47. Ojo, O. A. *et al.* Diabetes mellitus: From molecular mechanism to pathophysiology and pharmacology. *Medicine in Novel Technology and Devices* **19**, 100247 (2023).
48. Batool, S. *et al.* Delving the role of the ameliorative effects of *Caralluma tuberculata* NE Br. (*Apocynaceae*) on diabetes and its effect on the organs weight of alloxan-induced adult male mice. *Polish Journal of Environmental Studies* **33**, (2024).
49. Kashtoh, H. & Baek, K.-H. New insights into the latest advancement in α-amylase inhibitors of plant origin with anti-diabetic effects. *Plants* **12**, 2944 (2023).
50. Khan, H. A. *et al.* Green synthesis of silver nanoparticles from plant *Fagonia cretica* and evaluating its anti-diabetic activity through indepth in-vitro and in-vivo analysis. *Frontiers in Pharmacology* **14**, 1194809 (2023).
51. Rehman, G. *et al.* Green synthesis and characterization of silver nanoparticles using *Azadirachta indica* seeds extract: in vitro and in vivo evaluation of anti-diabetic activity. *Pharmaceuticals* **16**, 1677 (2023).
52. Debnath, G. *et al.* Green synthesis of silver nanoparticles using mushroom extract of *Pleurotus giganteus*: characterization, antimicrobial, and α-amylase inhibitory activity. *BioNanoSci.* **9**, 611–619 (2019).
53. Balan, K. *et al.* Antidiabetic activity of silver nanoparticles from green synthesis using Lonicera japonica leaf extract. *RSC Advances* **6**, 40162–40168 (2016).
54. Diallo, F. *et al.* Green synthesis and anti-inflammatory activity of silver nanoparticles based on leaves extract of *Aphania senegalensis*. *Biochemistry Research International* **2024**, 3468868 (2024).
55. Singh, P. *et al. In vitro* anti-inflammatory activity of spherical silver nanoparticles and monodisperse hexagonal gold nanoparticles by fruit extract of *Prunus serrulata* : a green synthetic approach. *Artificial Cells, Nanomedicine, and Biotechnology* 1–11 (2017) doi:10.1080/21691401.2017.1408117.
56. Abdelhafez, O. H. *et al.* Anti-inflammatory potential of green synthesized silver nanoparticles of the soft coral nephthea sp. supported by metabolomics analysis and docking studies. *IJN* **Volume 15**, 5345–5360 (2020).